JOURNAL OF GEOPHYSICAL RESEARCH, VOL. 105, NO. A12, PAGES 27,251–27,259, DECEMBER 1, 2000

The origin and development of the May 1997 magnetic cloud

D. F. Webb,[1,2] R. P. Lepping,[3] L. F. Burlaga,[3] C. E. DeForest,[4] D. E. Larson,[5]
S. F. Martin,[6] S. P. Plunkett,[7] and D. M. Rust[8]

Abstract. A complete halo coronal mass ejection (CME) was observed by the SOHO Large-Angle and Spectrometric Coronagraph (LASCO) coronagraphs on May 12, 1997. It was associated with activity near Sun center, implying that it was aimed earthward. Three days later on May 15 an interplanetary shock and magnetic cloud/flux rope transient was detected at the Wind spacecraft 190 R_E upstream of Earth. The long enduring southward magnetic fields associated with these structures triggered a geomagnetic storm. The CME was associated with a small coronal arcade that formed over a filament eruption with expanding double ribbons in $H\alpha$ emission. The flare was accompanied by a circular EUV wave, and the arcade was flanked by adjacent dimming regions. We surmise that these latter regions marked the feet of a flux rope that expanded earthward into the solar wind and was observed as the magnetic cloud at Wind. To test this hypothesis we determined key parameters of the solar structures on May 12 and compared them with the modeled flux rope parameters at Wind on May 15. The measurements are consistent with the flux rope originating in a large coronal structure linked to the erupting filament, with the opposite-polarity feet of the rope terminating in the depleted regions. However, bidirectional electron streaming was not observed within the cloud itself, suggesting that there is not always a good correspondence between such flows and ejecta.

1. Introduction

The May 12-15, 1997, event is probably the most unambiguous example of the geoeffectiveness of a halo coronal mass ejection (CME) observed to date. The halo CME completely surrounded the occulting disks of the Large-Angle and Spectrometric Coronagraph (LASCO) coronagraphs and was associated with the only major flare on this day, in active region 8038 just north of central meridian. This region had appeared as a new, rapidly developing region of new-cycle polarity on this rotation. It was the only active center on the entire disk and the site of all flaring activity for several days before and after May 12. The X-ray flare had a smooth long-duration (LDE) profile resulting from emission from a small, bright arcade that formed over a classic filament eruption with expanding double ribbons in $H\alpha$ emission. The arcade was flanked northeast and southwest by two dimming regions of the transient coronal hole type. The flare was also accompanied by a circular EUV wave. All of these transient features have been found in other studies to be well associated with CMEs.

Mimicking the quiet state of the Sun, the solar wind as observed near Earth also had been in a relatively simple and quiet state for about two weeks prior to May 15. A sector boundary crossing occurred on May 11 and possibly late on May 13, and the May 15 transient occurred on the leading edge of a modest, recurring high-speed stream. Therefore, the relatively quiet solar and interplanetary background into which this event was injected permits unambiguous identification and tracking of the surface activity, the halo CME, the magnetic cloud transient at 1 AU, and the geomagnetic storm, and this background makes the analysis and modeling of the underlying physics relatively simple.

In this paper we attempt to understand the origins and development of the CME and magnetic flux rope by measuring and comparing the following parameters of the erupting filament, arcade, and CME at the Sun with the observed magnetic cloud and modeled flux rope at 1 AU: the orientation and overall geometry; the chirality, that is, left- or right-handedness in magnetic helicity; the total magnetic flux; and the speeds. In section 2 we discuss the solar observations applicable to these measurmeents. In section 3 we describe the solar wind observations at Wind at 1 AU and the flux rope modeling, and in the section 4 we summarize and discuss the results.

2. Solar Observations

The important coronal observations of the May 12 event in the EUV with the Solar and Heliospheric Observatory (SOHO) Extreme Ultraviolet Imaging Telescope (EIT) and in white

[1] Institute for Scientific Research, Boston College, Chestnut Hill, Massachusetts.
[2] Also at Air Force Research Laboratory, Hanscom Air Force Base, Massachusetts.
[3] Laboratory for Extraterrestrial Physics, NASA Goddard Space Flight Center, Greenbelt, Maryland.
[4] Center for Space Science and Astrophysics, Stanford University, Stanford, California..
[5] Space Sciences Laboratory, University of California, Berkeley.
[6] Helio Research, Inc., La Crescenta, California.
[7] University Space Research Association, Naval Research Laboratory, Washington, D.C.
[8] Applied Physics Laboratory, Johns Hopkins University, Laurel, Maryland.

Paper number 2000JA000021.
0148-0227/00/2000JA000021$09.00

light with the LASCO instruments have been described in papers by *Thompson et al.* [1998] and *Plunkett et al.* [1998]. The halo CME on May 12 completely surrounded the occulting disk and was first seen in LASCO C2 at 0630 UT (see the images in the *Plunkett et al.* paper). Although the CME contained expanding structure symmetrically surrounding the occulting disk, the structures were brightest over the NE and WSW limbs and generally brighter to the north than to the south, as might be expected for a source region north of Sun center. However, previous studies have shown that associated surface features, such as active regions, flares, and filament eruptions, are often offset from the central axis of a CME, and the CME itself can bend toward the equator as it moves outward. Thus, despite its association with region 8038, it seems reasonable that the May 12 CME formed near the center of the disk.

Height-time plots of the leading edge of the CME at several position angles around the disk yielded similar constant speeds of 250 ± 20 km s^{-1}. This represents an expansion speed of the sides of the event as it is projected on the skyplane. *Plunkett et al.* [1998] estimated a true frontal speed (i.e., toward Earth) of ~ 600 km s^{-1}. Extrapolation of the height-time plots back to Sun center suggests a CME onset time between 0430 and 0500 UT, consistent with the onset time of 0442 UT of the only major flare on this day, in active region 8038 at N21°W08°. The X-ray flare peaked at 0455 UT (GOES flux level of C1.3 = 1.3 x 10^{-6}) and had a smooth long-duration profile lasting ~14 hours. This emission arose from a small, bright loop arcade that formed during the filament eruption.

In recent studies of halo CMEs from mid-December 1996 to mid-June 1997, all the halo CMEs were associated with small, long-duration coronal arcades and adjacent dimming regions [e.g., *Webb et al.,* 2000; *Hudson et al.,* 1998]. Such coronal arcades suggest the eruption and subsequent reconnection of the strongest magnetic field lines in the source regions associated with the CME and involve a simplification of the preevent magnetic structure. The dimming regions imply that material is evacuated from the low corona, and a few estimates show that the amount lost may be a significant fraction of the mass which later appears in the white light CME [see *Hudson and Webb,* 1997]. In some cases, such as the May 12 event, symmetric dimmings occur in regions which may be of opposite magnetic polarity flanking the central arcade. Such regions may mark the feet of a flux rope that is expanding into the solar wind, an idea supported by observations of associated magnetic clouds at Earth [e.g., *Smith et al.,* 1997; *Sterling and Hudson,* 1997].

The EIT instrument has now observed many EUV waves [*Thompson et al.,* 1999], which typically consist of a rim of enhanced coronal emission traveling quasi-radially across the disk from the flare site. They are considered to be caused by fast mode MHD waves that may or may not steepen into shock waves. The physical relationship of the EIT events to CMEs is not yet clear. On May 12 the propagation speed of the EIT wave, 245 ± 40 km s^{-1}, was close to that of the CME projected speed [*Thompson et al.,* 1998]. However, this may be a coincidence, since in other cases the speeds and locations of the waves do not match as well with associated CMEs.

EIT first observed the initial stages of the May 12 event at 0450 UT (Figure 1). The flare began in $H\alpha$ with a bright point at the base of a thin, dark filament that ran southward from the active region in a nearly N-S direction. As observed on a Solar Observing Optical Network Sunspot (SOONSPOT) movie for this day, this point first brightened at 0443 UT (Figure 2). Until that time, the filament had stretched southward from the center of the active region, but by 0444 UT a segment had rotated to the SSW, i.e., by ~60° in a counterclockwise direction (arrow in Figure 2). By 0446 UT the axis of the southern moving part was aligned ~80° from the N-S direction. Over the next several minutes the filament continued to move SW until it disappeared.

Erupting filaments and their associated coronal arcades are two specific solar features that can be used to estimate key characteristics of a flux rope observed in the solar wind. *Rust and Kumar* [1994], *Bothmer and Rust* [1997], *Martin,* [1998] and others have discussed comparisons between solar filaments and magnetic clouds. Although the physical relationship between an erupting filament and its overlying coronal structures and CME is still controversial, the inferred filament and arcade fields can be used to predict key components of the interplanetary flux rope, including its axial direction, chirality or handedness, and its pitch angle.

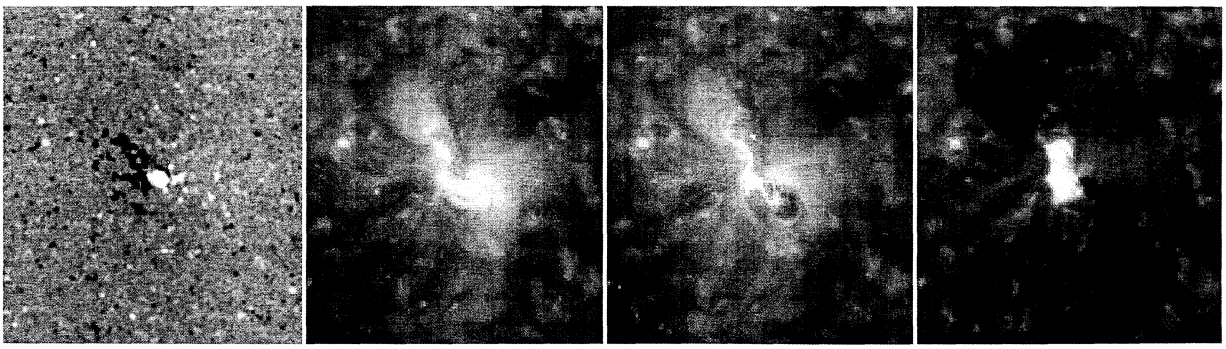

Figure 1. Example of surface activity associated with the May 12, 1997 halo coronal mass ejection (CME). Development of the coronal long-duration arcade and dual flanking dimming regions is shown. On left is a Solar and Heliospheric Observatory (SOHO)/Michelson-Doppler Imager (MDI) photospheric magnetogram. The other three images are 195Å Extreme Ultraviolet Imaging Telescope (EIT) images showing the following: at 0434 UT the preexisting active region; at 0450 UT the event onset; and at 0622 UT the fully developed arcade and dual dimmings. During the onset a filament was beginning to erupt from the southern part of the region. From *Webb et al.* [2000].

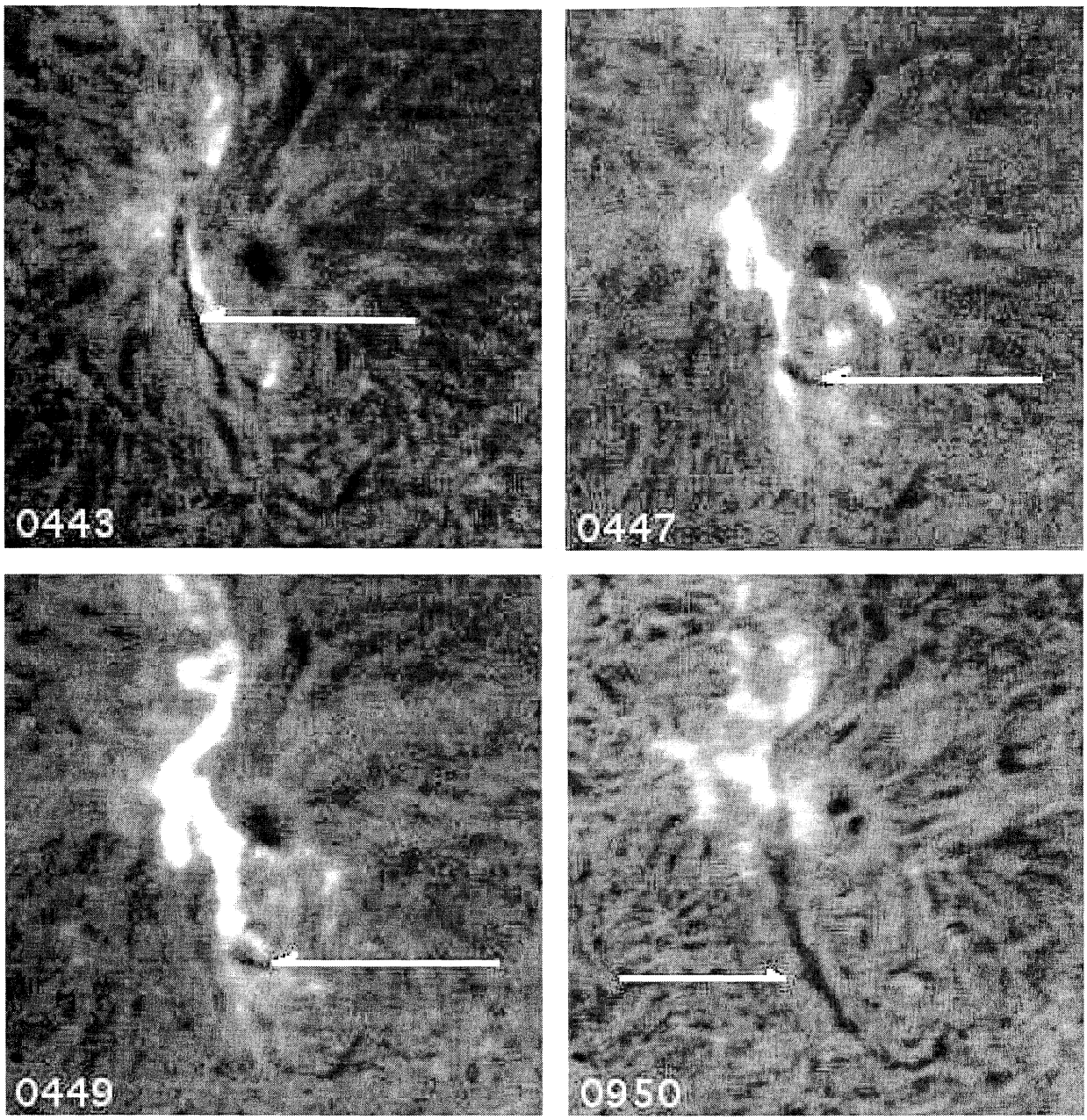

Figure 2. Sequence of Solar Observing Optical Network Sunspot (SOONSPOT) images of active region 8038 on May 12 showing evolution of flare and erupting filament. Arrows point to the following: 0443 UT, preexisting filament at event onset; 0447 and 0449 UT, motion of erupting filament toward southwest (note rotation toward an east-west alignment); 0950 UT, barb connecting to the filament that had reformed in channel after eruption.

Since the sign of the photospheric magnetic field in the ends of the filament was negative in the northeast and positive in the southwest, we conclude that the strong axial field of the filament at the onset of the event was directed northward and then rotated toward the east as the filament erupted. Measuring the filament orientation angle clockwise with 0° at due east, we get a range of estimates for the axial direction of the flux rope from 30°-55° to the NE. We also note that the twin dimming regions on opposite sides of the arcade lay roughly along a line which is at an angle of 55° north of the solar equator. If the filament continued to rotate after disappearing from $H\alpha$ and presumably moved outward, it could have entered the solar wind with its axial field directed nearly eastward.

Other parts of the filament remained rooted in the N-S filament channel as the two flare ribbons formed in the strong fields on either side. Seen faintly at 0500 UT in $H\alpha$ was a set of flare loops, i.e., "post-flare loops", that stretched across the filament channel horizontally and slightly southward from east to west. Their direction coincided with that of the loops seen later in EIT, 195Å (see Figure 1).

An unambiguous determination of the chirality of a filament

requires observations of often subtle magnetic features on opposite sides of the filament axis and of the direction of "barbs", or feet-like structures, relative to the filament axis. High quality $H\alpha$ images are necessary but not always available for a given event period. On May 12 there were several SOON frames of good quality that showed barbs in a filament that appeared in the channel after the flare. The barb orientation was that of a dextral filament (Figure 2). The filament was narrower and darker before the flare and did not exhibit clear individual fibrils. If we assume that the chirality of the erupted filament was the same as the filament that formed in the channel after the flare, then it was dextral. The left-handedness of the filament agrees with that expected for northern hemisphere filaments for this phase of solar cycle 23, and this handedness would produce a flux rope of the south-east-north (SEN) type as predicted by *Bothmer and Rust* [1997].

Our hypothesis is that the double dimming regions are the feet of the rising coronal flux loops that become the magnetic cloud at 1 AU, and the timing, location, and duration all seem consistent with this viewpoint. Thus the total magnetic flux in the feet of the flux loops should be consistent with that measured in the magnetic cloud at Wind. If we assume that the dimming regions are the result of the expansion of a single flux rope system, then we can use the near-simultaneous SOHO Michelson-Doppler Imager (MDI) and EIT images to locate the photospheric footpoints of the loop system in order to estimate the total magnetic flux in the loop system.

Figure 1 shows the photospheric magnetic field of the active region at 0628 UT. Careful measurements of the field before, during, and after the event showed no changes in the location or amount of total flux. We used an MDI image at 0454 UT, the nearest in time to the event onset, for the flux calculation. On May 12 the nearest EIT images to the MDI image were obtained at 0450, 0507, and 0524 UT. The 0524 UT image was the first on which the dimming regions were fully formed. We coaligned the three EIT images to the MDI image at 0454 UT. The alignment was done using the SOHO pointing data and checked by comparing corresponding brightenings in the EUV with magnetic flux concentrations in the photosphere. We then used difference image pairs between the EIT images to compare the darkened areas to the magnetic flux concentrations. The difference images are between 0507 and 0450 UT to show only the plasma that changed suddenly during the event. After compensating for projection effects, we concluded that the "masked" areas shown in Figure 3 best fit the possible magnetic footpoints of the dimming areas.

As expected, there was a rough balance in the active region between the amounts of positive (white) and negative (black) flux. Note that most of the flux associated with the SW footpoint area was positive and concentrated in the dominant leader sunspot. The measured flux in this area was less precise than that on the other side, because the mask boundary passed through the sunspot, where the field was large. Most of the flux to the NE was negative and more widely distributed. So, the presumed footpoints of the flux loop lay in opposite polarity regions, as expected, and the direction of the axial field in the loop was to the NE, in agreement with the inferences made from the filament observations. The measured amounts of flux in the NE and SW footpoints were estimated as -9×10^{20} and $+1.2 \times 10^{21}$ Mx, respectively, from which we estimate a total linked flux of $1.0 \pm 0.2 \times 10^{21}$ Mx. In section 3 we compare this flux with that calculated for the modeled flux rope observed at Wind. This flux along with other key results from the solar data on flux loop orientation, handedness, and speed is shown in Table 1.

3. Solar Wind Observations at 1 AU

Three days after the May 12 CME an interplanetary shock and magnetic cloud transient were observed by the Wind spacecraft 190 R_E upstream of Earth. Figure 4 is a stack plot of key IMF (Magnetic Field Investigation (MFI) experiment [*Lepping et al.*, 1995]) and plasma (Solar Wind Experiment (SWE) [*Ogilvie et al.*, 1995] and 3-D Plasma and Energetic Particle Investigation (3DP) [*Lin et al.*, 1995] instruments) parameters from the Wind spacecraft for May 14-17, 1997. An interplanetary shock arrived at Wind on May 15 at 0115 UT, followed 8 hours later by the magnetic cloud. The vertical dashed lines in Figure 4 mark the shock and the front and rear boundaries of the flux rope modeled by the MFI team.

Before the cloud's arrival, Wind was well upstream (~190 R_E) of Earth and in very slow speed solar wind. The plasma density ranged from 10 to 20 cm^{-3} and the proton temperature ranged from 1.5 to 6.0 eV. The electron heat flux was in the opposite direction to the magnetic field. This implies that the electrons were on field lines that pointed into the corona, which is consistent with the magnetic field direction (θ~300° or generally toward the Sun).

Just prior to the shock arrival, the heat flux electrons became more bidirectional, and there was an increase in these electrons traveling parallel to the magnetic field, most likely energetic electrons coming from the impending shock. The shock itself

Table 1. Comparison of Key Parameters of Solar Event and Modeled Flux Rope at 1 AU

Parameter	Solar	Flux Rope
Projected orientation	45° NE of equator 30°-55° NE (range) 55° axis of dimmings Filament rotates toward E-W	-11° ecliptic latitude 108° ecliptic longitude S-E-N type
Handedness	left	left
Magnetic flux	1.0×10^{21} Mx (dimmings)	7.35×10^{20} Mx (axial)
Speed	~600 km s^{-1} (CME front)	550 km s^{-1} (travel time) 450 km s^{-1} (cloud mean) 430-500 km s^{-1} (cloud range)

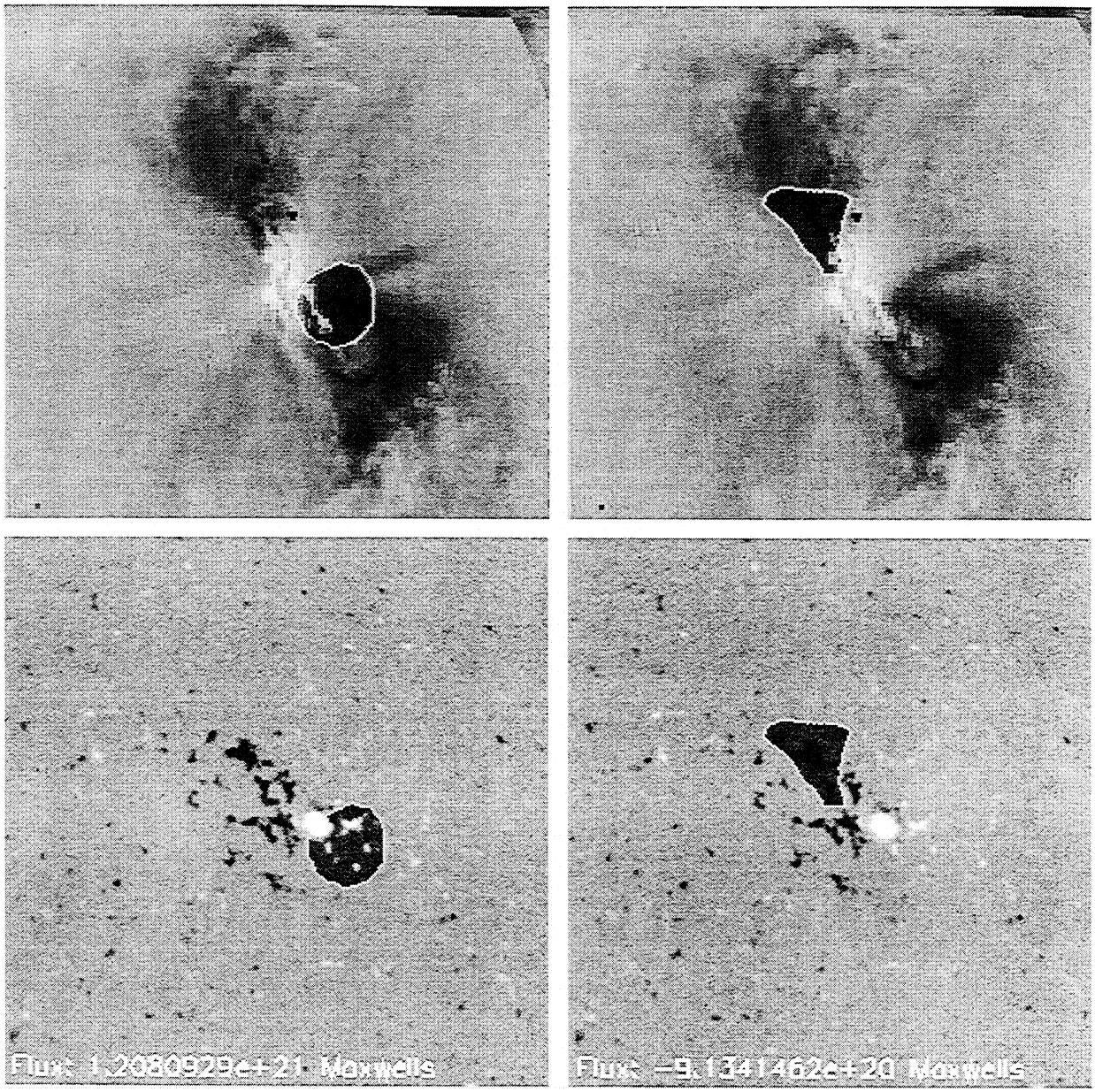

Figure 3. (Top) EIT difference image (0507 UT–0450 UT) and (bottom) MDI image (0454 UT). Superposed are the area masks which were used to estimate total magnetic flux at the assumed footpoints of erupting loop system. Masks used for the southwest (left) and northeast (right) dimming regions.

(see the paper of D. Berdichevsky et al., Interplanetary fast shocks and drivers observed through the twenty-third solar minimum by Wind over its first 2.5 years, submitted to Journal of Geophysical Research, 1999) had a surface normal that was very close (within 6°) to perpendicular to the cloud's axis, as expected if it were being driven by the CME/cloud. This approximately orthogonal relationship between the shock normal and a cloud axis has been observed for other cases.

After the shock arrived at Wind, the plasma density, temperature, and velocity all increased sharply. The plasma signatures that best mark the cloud onset occurred at 0950 UT. At this time the proton temperature decreased sharply, and the heat flux direction, relative to the field direction, changed sign from negative to positive, where it remained throughout the cloud. The period between the shock and the cloud onset was a turbulent region usually considered to consist of compressed ambient solar wind material and draped ambient IMF. However, some of these structures were possible overlying preexisting fields that might be ejected as part of the CME, i.e., that lie between the shock and the coronal cavity/magnetic cloud [*Tsurutani et al.,* 1998].

The plasma observations at Wind showed the following: (1) Unlike the earlier January 1997 halo CME [*Burlaga et al.,* 1998; *Webb et al.,* 1998], there was no high-density material or

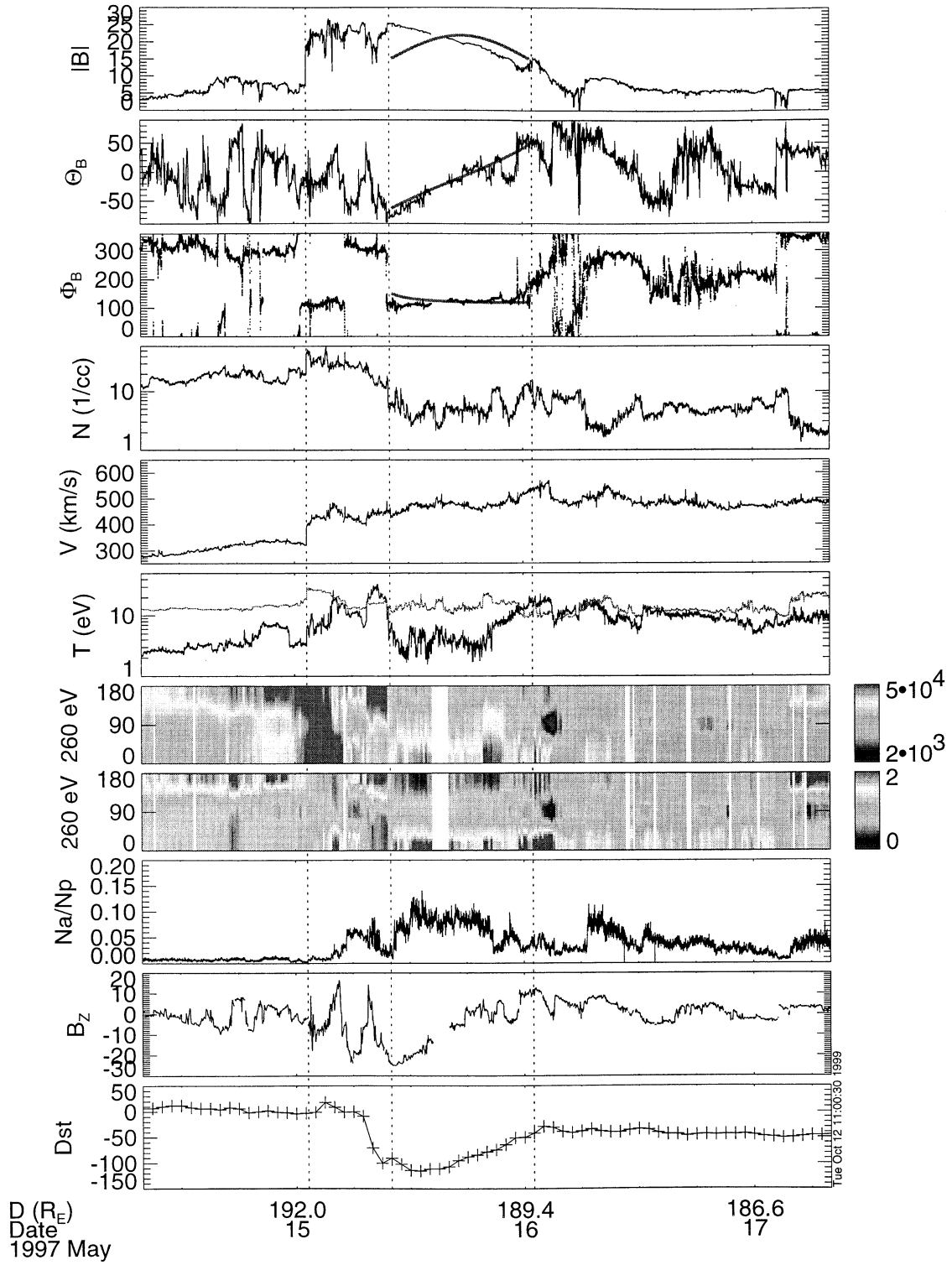

Figure 4. Time variations of key interplanetary magnetic field (IMF) and plasma parameters from Wind spacecraft for May 14-17, 1997. From top to bottom: magnetic field amplitude B, polar angle θ, azimuthal angle ϕ, plasma proton density N, bulk velocity V, proton and electron temperatures T, pitch angle distributions of 260 eV electrons in absolute flux and normalized to field direction (0° is pointed away from Sun and 180° is toward), ratio of alpha to proton particles *Na/Np*, N-S IMF component B_z (GSM coordinates), and *Dst* index at Earth. Shock arrived on May 15 at 0115 UT followed 9 hours later by the magnetic cloud. Vertical dashed lines denote shock and front and rear boundaries of flux rope modeled by the Magnetic Fields Investigation (MFI) team.

unusual ion charge states during the May event. Thus it is unlikely that the filament itself was encountered by Wind. (2) As is typical, the proton temperature was low within the cloud. (3) The helium abundance, a signature of ejecta, was enhanced within the cloud. (4) The electron temperature was typical of the undisturbed solar wind. (5) Bidirectional electron flux was not observed within the cloud itself. This might imply that the cloud was not connected to the Sun at both ends, but bidirectional flows are often not present or only occasionally present within magnetic clouds [e.g., *Gosling et al.,* 1995]. (6) Bidirectional flows were observed within the shocked plasma following the shock but before the onset of the cloud.

The main interplanetary signature corresponding to the solar event was an IMF magnitude enhancement on May 15 and 16 with a duration of ~ 3/4 days. It had the typical field and plasma signature of a magnetic cloud, i.e., a smoothly changing field direction and depressed proton temperature compared to the ambient as well as the enhanced field magnitude. There were strong north to south fields in the compressed region behind the shock and then mostly south to north fields in the cloud itself.

The magnetic field configuration of a magnetic cloud at 1 AU has been shown to be force-free [*Goldstein,* 1983; *Marubashi,* 1986] to a very good approximation. A magnetic cloud's geometry is that of a nested set of helical field lines confined to a flux tube curved on a large scale [*Farrugia et al.,* 1997], i.e., a curved flux rope, whose endpoints should be anchored back at the Sun for some finite time. For modeling purposes the cloud is usually well approximated locally by cylindrical symmetry. The pitch angle of the internal helical field lines increases with increasing distance from the axis of the magnetic cloud, such that the field is aligned with the axis of symmetry at the position of the axis and perpendicular to it on the cloud's boundary. An analytical approximation for this field configuration and the one employed here [*Lepping et al.,* 1990] is the static, constant-alpha (where $\mathbf{J} = \alpha \mathbf{x} \mathbf{B}$), force-free, cylindrically symmetric configuration [*Burlaga,* 1988], given by the Lundquist solution of $\nabla^2 \mathbf{B} = -\alpha^2 \mathbf{B}$, resulting from assuming $\mathbf{J} = \alpha \mathbf{B}$ and Maxwell's equations [*Lundquist,* 1950]. More accurate models consider the possibility that the magnetic cloud expands as it moves away from the Sun [e.g., *Burlaga et al.,* 1981] and/or consider the possibility of a violation of cylindrical symmetry [*Lepping et al.*, 1998]. Models of expanding magnetic clouds are reviewed by *Burlaga* [1995] and *Osherovich and Burlaga* [1997]. It is not expected that most of the seven model-produced parameter values obtained from *Lepping et al.'s* [1990] model will suffer markedly by our ignoring expansion or possible ellipticity in this case, especially those important to us such as handedness, polarity, or axial alignment.

Lepping et al.'s [1990] method of solution employs a least squares fit to the *Lundquist* [1950] solution to the 1-hour average observations of the field after unit normalization. A linear adjustment of field magnitude is then made to account for the spacecraft typically not passing through the cloud's axis. The boundaries of the May 15 cloud were chosen on the basis of the magnetic field profile, as well as on the (depressed) proton plasma beta profile, with slight boundary-time adjustments according to the quality of various trial fits, as measured by χ^2 (= 0.021) and the symmetry of the competing solutions. Both measures indicated that the final fit was judged to be good.

The cloud's best fit interval was chosen to be May 15, 1000 UT, to May 16, 0100 UT, a 15-hour duration typical of magnetic clouds at 1 AU. The central axis of the cloud had a longitude and latitude in GSE coordinates of 108° and -11°, respectively, and its helical field was left-handed. These values are typical of magnetic clouds measured in the Wind data, which have axial longitudes clustering at 80° and latitudes confined within 5° to the ecliptic plane. The left-handedness of the rope agrees with that expected for this phase of solar cycle 23 and was of the south-east-north (SEN) type as predicted by *Bothmer and Rust* [1997].

Other model-estimated quantities we determined were the following: a cloud radius of 0.103 AU, an axial field strength of 22.6 nT, an asymmetry factor of 6.7 (a measure of how far the peak B_o is from the center of the analysis interval; scale is 0=close, 100=far), the closest approach with respect to the cloud's radius (or impact parameter) of 0.20, and an axial magnetic flux of 7.35 x 10^{20} Mx. The axial field strength was significantly stronger than the average estimated axial field strengths ($<B_o>$) of 28 modeled Wind magnetic clouds of 16.4 nT, and the axial flux was about three-fourths that of the average cloud. A schematic drawing of the flux rope, including our estimate of its dimensions and orientation with respect to the ecliptic plane and the Sun-Earth line at the time of passage by Wind, is presented as Figure 5.

The travel time between the solar onset of the surface event and the cloud onset time at 1 AU was 76 hours, yielding an average transit speed of 548 km s^{-1}. This agrees well with the estimated speed of the CME front (section 2) of 600 km s^{-1}. The transit time can also be compared to the in situ solar wind speed within the cloud, which increased from 430 km s^{-1} at the front to 500 km s^{-1} at its rear, for an average speed across the cloud of 450 km s^{-1}. The increasing speed profile through the cloud is somewhat unusual; clouds at 1 AU are often still expanding [e.g., *Osterovich and Burlaga,* 1997]. Although there were apparently no nearby polarity sector boundaries, this cloud apparently was being compressed from behind by a high-speed stream.

Finally, the May 15 transient was associated with a moderate storm which reached a minimum *Dst* of -115 nT at 1300 UT. As in many of the halo CME/storm events during this post minimum period [*Webb et al.,* 2000], the May 15 storm closely matched the periods of strong, sustained southward fields both in the turbulent region between the shock and cloud and in the cloud itself (Figure 4, bottom panel).

4. Results and Discussion

The halo CME observed by LASCO on May 12, 1997, was associated with a long-lived coronal arcade just north of Sun center, a filament eruption, a circular EUV wave, and adjacent coronal dimming regions flanking the arcade. Three days later an interplanetary shock and magnetic cloud were detected at the Wind spacecraft upstream of Earth. Intense southward magnetic fields in these structures triggered a geomagnetic storm. We surmise that the transient dimming regions at the Sun marked the feet of a flux rope that expanded earthward into the solar wind and was observed as the magnetic cloud at Wind. To test this hypothesis we determined key parameters of the solar structures on May 12 and compared them with the modeled flux rope parameters at Wind on May 15 (Table 1). The estimated frontal speed of the CME was consistent with

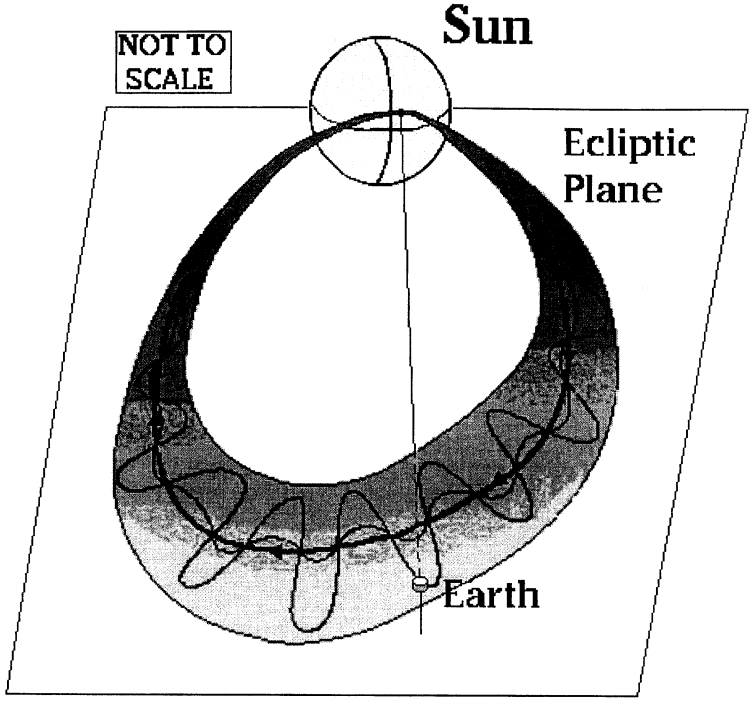

Figure 5. Schematic drawing of modeled flux rope, including estimate of its dimensions and orientation with respect to the ecliptic plane; the axis of the cloud lay nearly in the ecliptic plane and pointed toward the east. Also drawn is the Sun-Earth line at time of cloud passage by Wind near the L1 point.

the travel time between event onset at the Sun and cloud onset at 1 AU. The Wind observations show that the central axis of a flux rope with left-handed helicity passed near the spacecraft on May 15 starting at 1000 UT. The rope axis lay nearly in the ecliptic plane and pointed toward the east, in agreement with the inferences from the solar observations. The magnetic flux in the rope was within a factor of 2 of that estimated in the loop footpoints at the Sun. Thus the measurements are consistent with the flux rope originating in a large coronal structure overlying and tied to the erupting filament, with the opposite-polarity feet of the rope terminating in the depleted regions.

The flux rope passed Wind with its axial field nearly along the $+Y$(GSE) direction, i.e., orthogonal to the Sun-Earth line. The cloud axis passed slightly below the ecliptic plane. How could the cloud come from a solar source region that was north of the solar equator? Remember that the moving part of the erupting filament was directed toward the solar equator and rotating toward alignment with it. The filament was probably only a small portion at the base of the much larger mass ejection, which in white light appeared to arise from near disk center. Thus we feel the solar observations are consistent with the flux rope orientation and geometry at 1 AU.

The present study suggests that high-quality observations of the solar signatures of a CME/flux rope eruption can be used to predict important features of the subsequent interplanetary disturbance at Earth. In particular, the axial orientation of the magnetic field and the variation in the N-S component of the field in a magnetic cloud striking Earth can be accurately inferred from the properties of the corresponding filament eruption. In addition, with a suitable model assuming self-similar expansion, even the magnitude of the field in the magnetic cloud can be inferred from photospheric magnetic field observations and coronal observations of the transient dimming regions astride the filament.

Acknowledgments. This study is a collaboration from the ISTP/IACG (International Solar-Terrestrial Physics/Interagency Consultive Group) workshop on a Global Picture of Solar Eruptive Events held at NASA/GSFC in April 1999. SOHO is an international collaboration between NASA and ESA and is part of the ISTP. We are grateful to Alan Kiplinger of NOAA, Diana Taggart, Adam Szabo and Daniel Berdichevsky of GSFC, and K. Ogilvie, the Wind SWE P.I., for providing data or analyses for this study. D.F.W. was supported by Air Force contract AF19628-96-K-0030, by AFOSR grant AF49620-98-1-0062, and by NASA grant NAGW-4578; D.E.L. was supported by NASA grant NAG5-6928; D.M.R. was supported by NASA grant NAG5-7921; and S.P.P. was supported by NASA grant NAG5-8116 and NASA contract S-86760-E.

Janet G. Luhmann thanks Charles W. Smith, John T. Steinberg, and another referee for their assistance in evaluating this paper.

References

Bothmer, V,. and D.M. Rust, The field configuration of magnetic clouds and the solar cycle, in *Coronal Mass Ejections, Geophys. Monogr. Ser.*, vol. 99, edited by N. Crooker et al., p. 139, AGU, Washington, D.C., 1997.

Burlaga, L.F., Magnetic clouds: Constant alpha force-free configurations, *J. Geophys. Res., 93*, 7217, 1988.

Burlaga, L.F., *Interplanetary Magnetohydrodynamics*, Oxford Univ. Press, New York, 1995.

Burlaga, L.F., E. Sittler, F. Mariani, and R. Schwenn, Magnetic loop behind an interplanetary shock: Voyager, Helios and IMP-8 observations, *J. Geophys. Res., 86*, 6673, 1981.

Burlaga, L., et al., A magnetic cloud containing prominence material: January 1997, *J. Geophys. Res., 103*, 277, 1998.

Farrugia, C.J., L.F. Burlaga, and R.P. Lepping, Magnetic clouds and the quiet-storm effect at Earth, in *Magnetic Storms*, *Geophys. Monogr. Ser.*, vol. 98, eds. B.T. Tsurutani, W.D. Gonzales, and Y. Kamide, p. 91, AGU Washington, D.C., 1997.

Goldstein, H., On the field configuration in magnetic clouds, in *Solar Wind Five,* edited by M. Neugebauer, *NASA Conf. Publ. 2280*, 731, 1983.

Gosling, J.T., J. Birn, and M. Hesse, Three-dimensional magnetic reconnection and the magnetic topology of coronal mass ejection events, *Geophys. Res. Lett., 22*, 869, 1995.

Hudson, H.S., and D.F. Webb, Soft X-ray signatures of coronal ejections, in *Coronal Mass Ejections*, *Geophys. Monogr. Ser.*, vol. 99, edited by N. Crooker, J. Joselyn, and J. Feynman , p. 27, AGU, Washington, D.C., 1997.

Hudson, H.S., J.R. Lemen, O.C. St. Cyr, A.C. Sterling, and D.F. Webb, X-ray coronal changes during halo CMEs, *Geophys. Res. Lett., 25*, 2481, 1998.

Lepping, R.P., J.A. Jones, and L.F. Burlaga, Magnetic field structure of interplanetary magnetic clouds at 1 AU, *J. Geophys. Res., 95*, 11,957, 1990.

Lepping, R.P., et al., The Wind magnetic field investigation: The Global Geospace Mission, *Space Sci. Rev., 71*, 207, 1995.

Lepping, R.P., D. Berdichevsky, A. Szabo, M. Goodman, and J. Jones, Modification of magnetic cloud model: Elliptical cross-section (abstract), *Eos Trans. AGU, 79*(45), Fall Meet. Suppl., F696, 1998.

Lin, R.P., et al., A three-dimensional plasma and energetic particle investigation for the Wind spacecraft: The Global Geospace Mission, *Space Sci. Rev., 71*, 125, 1995.

Lundquist, S., Magnetohydrostatic fields, *Ark. Fys., 2*, 361, 1950.

Martin, S.F., Filament chirality: A link between fine-scale and global patterns, in *New Perspectives on Solar Prominences*, edited by D. Webb, D. Rust, and B. Schmieder, *ASP Conf. Ser.,* vol.150, ASP, p. 419, San Francisco, 1998.

Marubashi, K., Structure of the interplanetary magnetic clouds and their solar origins, *Adv. Space Res., 6*(6), 335, 1986.

Ogilvie, K.W., et al., SWE, A comprehensive plasma instrument for the Wind spacecraft: The Global Geospace Mission, *Space Sci. Rev., 71*, 55, 1995.

Osherovich, V., and L.F. Burlaga, Magnetic clouds, in *Coronal Mass Ejections*, *Geophys. Monogr. Ser.*, vol. 99, edited by N. Crooker, J. Joselyn, and J. Feynman, p. 157, AGU, Washington, D.C., 1997.

Plunkett, S.P., B.J. Thompson, R.A. Howard, D.J. Michels, O.C. St. Cyr, S.J. Tappin, R. Schwenn, and P.L. Lamy, LASCO observations of an Earth-directed coronal mass ejection on May 12, 1997, *Geophys. Res. Lett., 25*, 2477, 1998.

Rust, D.M., and A. Kumar, Helical magnetic fields in filaments, *Sol. Phys., 155*, 69, 1994.

Smith, Z., S. Watari, M. Dryer, P. Manoharan, and P. McIntosh, Identification of the solar source for the 18 October 1995 magnetic cloud, *Sol. Phys., 171*, 177, 1997.

Sterling, A.C., and H.S. Hudson, Yohkoh SXT observations of X-ray "dimming" associated with a halo coronal mass ejection, *Astrophys. J., 491*, L55, 1997.

Thompson, B.J., S.P. Plunkett, J.B. Gurman, J.S. Newmark, O.C. St. Cyr, and D.J. Michels, SOHO/EIT observations of an Earth-directed coronal mass ejection on May 12, 1997, *Geophys. Res. Lett., 25*, 2465, 1998.

Thompson, B.J. et al., The correspondence of EUV and white light observations of coronal mass ejections with SOHO EIT and LASCO, in *Sun-Earth Plasma Connections*, *Geophys. Monograph Ser.,* vol. 109, edited by J. L. Burch, R. L. Carovillano, and S. K. Antiochos, p. 31,, AGU, Washington, D.C., 1999.

Tsurutani, B.T., et al., The January 10, 1997 auroral hot spot, horseshoe aurora and first substorm: A CME loop?, *Geophys. Res. Lett., 25*, 3047, 1998.

Webb, D.F., E.W. Cliver, N. Gopalswamy, H.S. Hudson, and O.C. St. Cyr, The solar origin of the January 1997 coronal mass ejection, magnetic cloud and geomagnetic storm, *Geophys. Res. Lett., 25,* 2469, 1998.

Webb, D.F., E.W. Cliver, N.U. Crooker, O.C. St. Cyr, and B.J. Thompson, Relationship of halo coronal mass ejections, magnetic clouds, and magnetic storms, *J. Geophys. Res.,, 105*, 7491, 2000.

L. F. Burlaga and R. P. Lepping, Laboratory for Extraterrestrial Physics, NASA Goddard Space Flight Center, Greenbelt, MD 20771.

C. E. DeForest, Center for Space Science and Astrophysics, Stanford University, Stanford, CA 94305.

D. E. Larson, Space Sciences Laboratory, University of California, Berkeley, CA 94720.

S. F. Martin, Helio Research, Inc., 5212 Maryland Ave., La Crescenta, CA 91214.

S. P. Plunkett, USRA, Code 682, NASA Goddard Space Flight Center, Greenbelt, MD 20771.

D. M. Rust, APL, Johns Hopkins University, Laurel, MD 20723.

D. F. Webb, AFRL/VSBS, 29 Randolph Road, Hanscom AFB, MA 01731-3010. (David.Webb@hanscom.af.mil)

(Received January 24, 2000; revised January 25, 2000;
accepted February 7, 2000.)